Breathing, speaking, coughing or sneezing: What drives transmission of SARS-CoV-2?

● V. Stadnytskyi (iD), P. Anfinrud (iD) & A. Bax (iD)

From the Laboratory of Chemical Physics, NIDDK, National Institutes of Health, Bethesda, MD, USA

Stadnytskyi V, Anfinrud P, Bax A. Breathing, speaking, coughing or sneezing: What drives transmission of SARS-CoV-2?. *J Intern Med* 2021; https://doi.org/10.1111/joim.13326

Abstract. The SARS-CoV-2 virus is highly contagious, as demonstrated by numerous well-documented superspreading events. The infection commonly starts in the upper respiratory tract (URT) but can migrate to the lower respiratory tract (LRT) and other organs, often with severe consequences. Whereas LRT infection can lead to shedding of virus via breath and cough droplets, URT infection enables shedding via abundant speech droplets. Their viral load can be high in carriers with mild or no symptoms, an observation linked to the abundance of SARS-CoV-2-susceptible cells in the oral cavity epithelium. Expelled droplets rapidly lose water through evaporation, with the smaller ones transforming into long-lived aerosol. Although the largest speech droplets can carry more virions, they are few in number, fall to the ground rapidly and therefore play a relatively minor role in transmission. Of more concern is small speech aerosol, which can descend deep into the LRT and cause severe disease. However, since their total volume is small, the amount of virus they carry is low. Nevertheless, in closed environments with inadequate ventilation, they can accumulate, which elevates the risk of direct LRT infection. Of most concern is the large fraction of speech aerosol that is intermediate-sized because it remains suspended in air for minutes and can be transported over considerable distances by convective air currents. The abundance of this speech-generated aerosol, combined with its high viral load in pre- and asymptomatic individuals, strongly implicates airborne transmission of SARS-CoV-2 through speech as the primary contributor to its rapid spread.

Keywords: aerosol, airborne transmission, infectious dose, SARS-CoV-2, speech droplet, superspreading events.

Introduction

The coronavirus disease 2019 (COVID-19) pandemic represents the most severe public health crisis of the last 100 years, both in terms of its human toll and economic cost. Even though the underlying pathogen, severe acute respiratory syndrome coronavirus 2 (SARS-CoV-2), is a member of the coronavirus family that has been studied extensively for many decades [1–4], the world was ill prepared to deal with its high degree of contagion combined with its broad spectrum of virulence. Regretfully, knowledge gained about the physical underpinnings of respiratory viral transmission after the 1918 Spanish flu pandemic, summarized in the 1955 textbook by Wells, was largely ignored by the public health community at the outset of the COVID-19 pandemic. In particular, it was well understood from the seminal work of Wells and Duguid [5,6] that the separate classification of respiratory droplets and aerosol is fundamentally flawed, as the vast majority of droplets convert into aerosol [7]. Nevertheless, this view persists even today and has led to serious misconceptions regarding the distance distribution of virus in air surrounding an infected person [8]. In this review, we use the word droplet to emphasize its liquid character when it is generated. Briefly, all respiratory aerosols start out as liquid droplets whose 95–99% aqueous fraction fully evaporates, which causes them to shrink to a size limited by the remaining non-volatile components. The resulting particles historically were named droplet nuclei, but are referred to as particles or respiratory aerosol in this review. Droplets with initial diameters in excess of *ca* 100 μm have a substantial probability of reaching the ground before their aqueous fraction fully evaporates. How long smaller particles will linger in the air, and how far they can spread depend on their size after dehydration.

As will be discussed, respiratory particles span a continuum of sizes and a corresponding continuum of airborne lifetimes, with the initial droplet size distribution strongly dependent on the respiratory activity that generates them. Importantly, SARS-CoV-2 not only remains viable for extended periods when airborne [9,10], but remains viable longer when fully desiccated than when maintained in a hydrated state [11], presumably due to chemical degradation in the aqueous environment.

Eventually, the vast majority of all emitted respiratory droplets deposit on solid surfaces. Doping of such fluids with fluorescent agents has revealed how their contents can be spread by touching, highlighting a potential pathway for pathogen transmission [12]. Although the importance of this fomite route has been well documented for numerous pathogens [13], its relevance for transmission of respiratory virus remains contested [14,15]. For example, the classic poker player study by Dick et al. [16] serves as a reminder of the low risk of fomite transmission of rhinovirus-16. When the poker player's air spaces were kept separate, twelve hours of passing chips and cards, described as 'saliva-soggy' at the end of the game, failed to transfer infection from eight rhinovirus-16-infected players to any of 12 disease-free recipients. In contrast, extensive transmission occurred when the players shared air. Still, the potential of resuspension in air of surface-deposited virus cannot be ignored [17,18], in particular in view of the extended viability of SARS-CoV-2 on inert surfaces [11]. The sometimes very high concentrations of virus in faecal matter raise the possibility of additional transmission pathways, possibly involving aerosolization of waste water in toilets [19] or drinking water contamination, especially in the third world. However, the viability of SARS-CoV-2 in water appears rather limited, where it is very susceptible to oxidants such as chlorine [20]. It is worth noting that viral RNA in untreated wastewater can be easily detected, which affords a sensitive probe for surveillance of community spread of the disease and the emergence of new variants [21,22].

Much debate has centred on the question of whether SARS-CoV-2 transmission is dominated by direct transfer of large droplets or through an airborne route involving small- to intermediate-sized aerosols that spend more than a few seconds in the air and dehydrate before being inhaled by a recipient. Whereas the direct droplet route may be expected to be comparably effective indoors and outdoors, the airborne route will be far more effective indoors, where the concentration of particles can accumulate over time. The observation that transmission in outdoor settings is at least an order of magnitude lower than indoors [23] strongly suggests that the airborne route is key. Indeed, consensus among aerosol experts has emerged that transfer of respiratory secretions through the air dominates the SARS-CoV-2 transmission pathway [24].

Respiratory droplets emitted while breathing, speaking/singing, coughing, and sneezing span a continuum of sizes that depend on their generation mechanism and their site of origin. The latter three types of droplets were the target of the classic slide deposition, microscope readout technology used more than 50 years ago [6,25,26], which is best suited for particles larger than 40 μm as smaller particles can drift far from the source before landing. The introduction of user-friendly and highly precise aerosol detection equipment, including aerodynamic particle sizers and optical particle counters [27], now allows straightforward measurement of both the quantity and size of small airborne particles over an instrument-limited range of *ca* 0.3–10 μm. The gap in the size range accessible to characterization by these methods is readily filled by light scattering techniques. For example, light scattering photographs of droplets emitted from the oral cavity revealed their abundance more than 80 years ago [28]. Recently, video recordings of light scattered from droplets generated during vocalization provided vivid illustrations of their abundance and wide range in size [29–32] (Fig. 1a). These videos afford not only an accurate count of emitted particles, but, when recorded in a sealed enclosure, can be used to estimate their airborne lifetimes, the majority of which were found to span many minutes (Fig. 1b) [33]. Compared with tabulations of particle sizes and number densities, these visually compelling recordings [30–32] better communicate to the public not only the enormous quantities of aerosol emitted by speaking, which are otherwise invisible to the naked eye, but also the attendant risks associated with speech.

Many insightful reviews discussing both the physical and medical aspects of aerosols in virus transmission have appeared since the start of the COVID-19 pandemic [34–40], discarding any residual doubt regarding the importance of the airborne
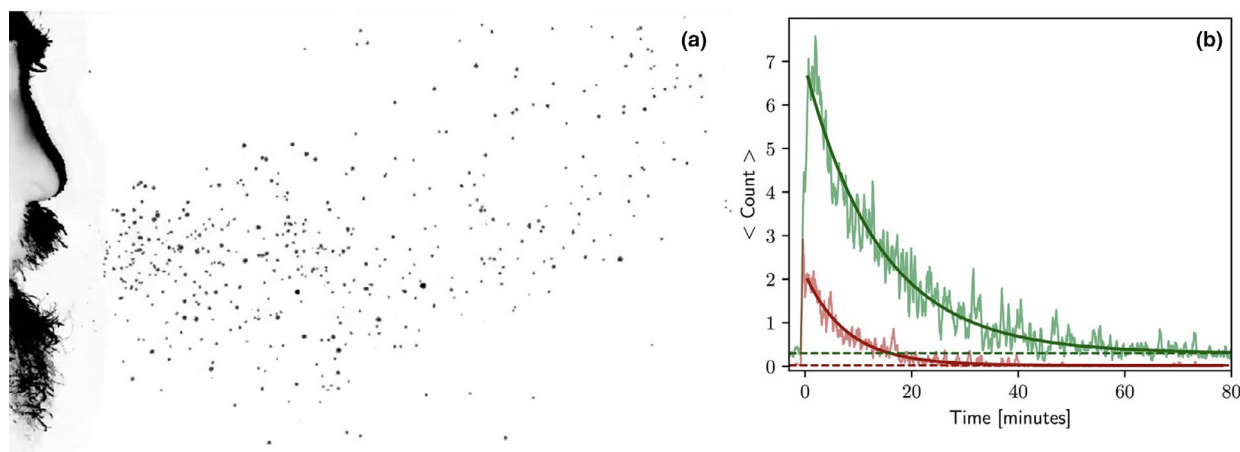
Fig. 1 *Analysis of speech droplets. (a) A single frame from a high-speed video recording of a person emitting speech droplets during vocalization. The video recording is available in [31], reprinted by permission of the American Association for Aerosol Research, www.aaar.org. (b) Chart of particle count per frame vs. time observed using light scattering. The particles were generated by a 25-s burst of repeatedly speaking the phrase 'stay healthy' in a loud voice into a 200-L cubic box. The red curve represents the top 25% in scattering brightness, with the remainder in green. The brighter fraction (red) decays with a time constant of 8 min, and the dimmer fraction (green) decays with a time constant of 14 min. From [33], reprinted by permission of PNAS, www.pnas.org.*

pathway [41]. The focus of the current review is on the interface between physics and medicine, including the relation between mechanisms and physical origins of virus emission at different stages of disease, and on the dual role of masks in both containing the spread of disease and mitigating its severity.
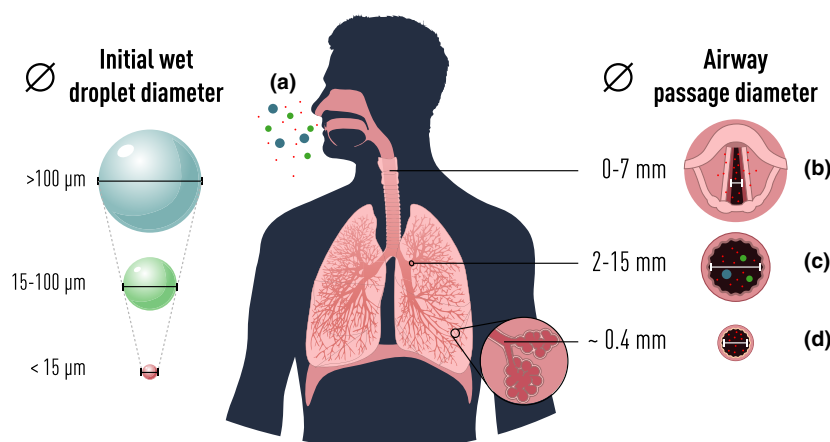
Generation of respiratory droplets

Respiratory droplets originate in the lungs, trachea, larynx and oral/nasal passages and consist of ≥95% water at the time they are first generated. The mechanisms responsible for their formation are tightly coupled to the physical dimensions and airflow speed within these sites. Activities that generate respiratory droplets are briefly reviewed below.

Breathing

The average resting adult respires about seven litres of air per minute or about 10,000 litres of air per day [42]. The volume of air inhaled during tidal breathing typically falls in the 0.5 to one litre range, representing only a small fraction of the average total lung capacity of about six litres. During inhalation, air passes through the oro- or nasopharynx, the larynx and trachea, the upper,

central and distal airways, and ultimately to the alveoli where blood–air O_2/CO_2 exchange takes place (Fig. 2). Below the trachea, the airways split 23 times with their total cross-sectional area being roughly preserved through the first five branchings, implying comparable velocities of air flow through these upper airways. Airways generated by the first 7 branchings correspond to the bronchi; subsequent branchings generate the bronchioles, which terminate in *ca* eight million alveolar ducts with channel diameters of about 0.4 mm [43]. These ducts connect to alveolar sacs housing *ca* 70 alveoli, each with a diameter of a few hundred microns [44]. Elastic fibres embedded in the walls of the alveoli, and distal airways allow their surfaces to stretch when they fill with air during inspiration, increasing their internal diameter, and to spring back during expiration when expelling the CO_2-rich air.

The inner surfaces of these airways are covered with respiratory tract lining fluid (RTLF). For the non-respiratory trachea, bronchi and bronchioles, which contain ciliated epithelial cells, this RTLF is two-layered. The periciliary liquid layer of the RTLF, with a thickness of about 5 μm, is of low viscosity, whereas the air-surface layer of *ca* 1-μm thickness is rich in cross-linked mucin proteins and of high-viscosity. To inhibit occlusion of the

Fig. 2 *Respiratory droplets emitted during exhalation, vocalizing, coughing or sneezing span a broad range of sizes that depend on the site of origin. Droplets are colour-coded according to their initial, fully hydrated diameter: red (<15 µm); green (15-100 µm); and blue (>100 µm). Once airborne, they shrink about threefold. (a) Largest droplets are generated during vocalization near the front of the oral cavity, where airflow is modulated by varying gaps between lips, tongue, and teeth. (b) Small droplets are generated by the vocal folds when vocalizing. (c) Rapid airflow through the central and upper airways during coughing, sneezing or sudden exhalation can produce a wide size distribution of droplets. (d) Transient closure of the distal airways is assumed to be responsible for the generation of small breath droplets.*

alveoli and the small diameter bronchioles in the distal airways, their RTLF is rich in pulmonary surfactants that lower the surface tension. Since the fluid contained in breath droplets is specific to the site where they are generated, analysis of their chemical composition and encapsulated biomarkers holds strong diagnostic potential for small airways disease [45,46].

While at rest, so-called tidal breathing creates airflow of a few metres per second in the trachea and upper airways. This airflow is close to the onset of turbulence, which can trigger the generation of breath droplets (see 'Coughing and sneezing' below). The number of breath droplets generated in the upper airways shows large person-to-person variation and can steeply increase upon viral infection [47], but can be reduced by increasing the RTLF surface tension through salt inhalation [48]. As air passes through the more numerous and narrower diameter central and terminal airways, it slows considerably and is expected to be laminar [43,49]. Consequently, the turbulent droplet extraction mechanism does not apply for these airways.

Despite the presence of pulmonary surfactant in the small terminal airways, they can become transiently occluded with RTLF, with deep exhalation increasing the number of occluded airways.

Subsequent inhalation creates a pressure differential across the occluded airway, and as the channel diameter expands, the length of the blockage shortens and forms a thin film that can burst and generate numerous small droplets [35]. These droplets are first drawn into the alveoli during inhalation and then forced out during exhalation [50–52]. Breath droplets generated by this mechanism span a size range from 0.01 to 2 micron in their hydrated state [53], whose size distribution is reasonably well described by a single lognormal centred at ca 0.7 micron [54].

Whereas the total liquid volume of exhaled breath particles in a healthy person at rest is typically very small ($\leq$ 15 pL/L air) [27], respired air volumes during aerobic exercise can be an order of magnitude larger. Combined with both deeper exhalation and proportionately higher airflow velocity through the airways, the number of breath droplets generated is expected to increase much more steeply than linear with respired air volume. Empirical observations of high virus transmission incidence in aerobic exercise facilities support this hypothesis [55,56].

Coughing and sneezing

Coughing and sneezing are widely recognized as an eruptive source of pathogen-containing droplets

and often manifest as symptoms of respiratory disease. Both are initiated by simultaneous closure of the glottis and contraction of the abdominal muscles [57]. The subsequent build-up of air pressure in the lungs is released by sudden opening of the glottis, resulting in expulsion of compressed air at speeds that can exceed 15 metres per second in the central and upper airways (Fig. 2c) [58]. At such high speeds, the airflow becomes turbulent, with friction between chaotic airflow and the lining of these airways generating RTLF waves (Fig. 3c) from which droplets can be dislodged through a variety of mechanisms [59].

Cough can be either voluntary or a protective reflex in response to stimulation of irritant receptors by foreign particles in the air passages. However, most studies reported in the literature focused on voluntary cough, which may differ substantially from reflex-driven cough. The common COVID-19 symptoms include 'dry cough' [60], that is a type of cough without the usual richness in phlegm but perhaps closer to that of a voluntary cough. Cough droplets span a very wide range of sizes from less than 1 μm to more than 100 μm, that is more than six orders of magnitude in volume [6,26,54].

Sneezing is a common reflex to cleanse irritants from the nasal cavities. During a sneeze, the soft palate and palatine uvula depress, while the back of the tongue elevates to partially close the passage to the mouth so that air ejected from the lungs may be expelled through the nose. In-depth studies of the mechanics of sneezing combined with high-speed video recording have generated revealing images of the quantities of droplets and the distances over which they are propelled [36]. The extreme air speeds associated with a sneeze result in turbulent flow that can dislodge RTLF and fluid lining from the oral and nasal passages (Fig. 3c). In contrast to several other types of respiratory tract infection, sneezing is not among the common symptoms of infection with SARS-CoV-2 [55,60]. Nevertheless, even if not triggered by the infection, a sneeze by a carrier will generate a large cloud of virus-laden respiratory fluid droplets [61].

Speaking and Singing

The acoustic waves generated during vocalization involve high-speed passage of air pressurized by the lungs past the mucosal epithelial layers of the vibrating vocal folds (Fig. 2b). These sounds are further modulated when air travels through narrow passages between the tongue, lips and teeth [62]. For example, enunciation of 'p' and 'b' involves parting of the lips, whereas 't' involves transient contact of the tongue and teeth. As these surfaces part, a fluid filament or film is formed between them. Air rushing by can break the filament or burst the film with the fluid fragmenting into droplets that join the airstream (Fig. 3a,b). Videography of droplet formation between parting lips provides a compelling visual illustration of this mechanism (Fig. 3e) [63]. Droplets generated in the oral cavity consist mostly of saliva and span a range of sizes comparable in quantity and size to those generated by coughing and sneezing (Duguid, 1946; Wells, 1955), with some droplets exceeding 100 μm [6,26]. Note that speech droplet measurements often involved continuous counting from 1 to 100, which lacks the droplet-rich 'p' and 'b' sounds. By contrast, regular speech includes these plosives and pauses that may involve wetting of the lips, both of which can significantly increase the droplet count.

High-speed laryngoscopic video recordings clearly demonstrate formation of fluid filaments between the separating vocal folds (Fig. 3d), which then fragment and form droplets. Moreover, airspeeds in a physical model of vocal folds [64] were found to be well in the turbulent range and may trigger additional dislodgment of surface fluid. During vocalization of a vowel sound, the vocal folds generate droplets at a rate of hundreds per second, which increase in number with loudness [65]. Droplets generated at the vocal folds by these mechanisms are mostly in the 1–5 μm size range and have a total volume of *ca* 1 pL per second [27], which is several orders of magnitude less than the volume of droplets formed at the front of the oral cavity while speaking, but several orders of magnitude more than breathing by a healthy person.

Respiratory aerosol risk assessment

Considering that respiratory aerosol constitutes the dominant mode of SARS-CoV-2 transmission, it is useful to assess the likelihood such particles are inhaled and the risk they pose upon inhalation. The probability of inhalation depends on many factors, including the airborne lifetime. Respiratory particles fall to the ground under the force of gravity at a rate that depends on their size. In stagnant air, a particle's sedimentation velocity is proportional to the square of its diameter. For example, a 100-μm droplet with a density of 1 g/cm^3 falls at a rate of

Filament breakage

Film bursting

**Turbulent droplet extraction**
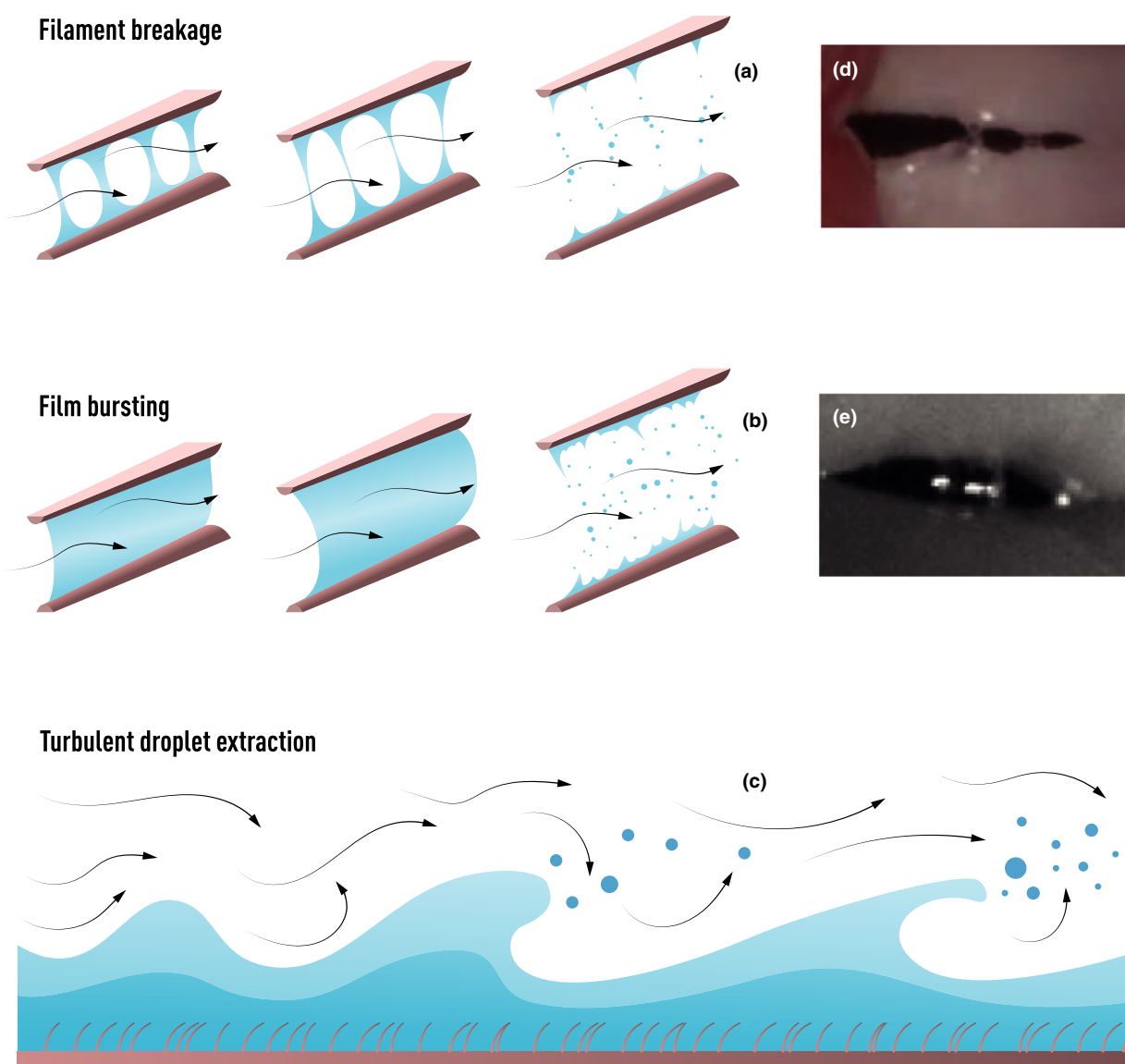
Fig. 3 *Mechanisms of respiratory droplet generation. Separation of two wetted surfaces creates filaments (a) or films of fluid (b) that become thinner as the surfaces separate; these filaments and films are ruptured by exhaled air, creating droplets that join the exhalation airflow (black arrows). These processes are operative in small diameter airways (during inhalation), at the vocal folds and in the oral cavity. (c) During rapid exhalation, coughing or sneezing, turbulent air flow creates instabilities at the air–fluid interface, causing wave formation in the mucosal layer that can result in droplet release through a variety of mechanisms, including film bursting, wave undercutting and shearing off the tops of roll waves [59]. (d) Example of filaments created between the vocal folds during vocalization, adapted from https://youtu.be/v9Wdf-RwLcs, which was produced by the University of Washington Speech and Hearing Clinic. (e) Example of a film forming between parting lips during speaking, adapted from a high-speed video recording [63].*

nearly 0.3 metres per second. Since respiratory droplets are mostly water (*ca* 95–99%), evaporation during their fall causes their diameter to shrink by roughly a factor of 3, which will slow their descent

by nearly an order of magnitude. The rate of droplet dehydration depends on size, the relative humidity (RH) of the surrounding air, the chemical potential of its salt-rich water and its temperature, which is

lowered by evaporative cooling of the droplet. Calculated airborne lifetimes that account for evaporation (Fig. 4a) show that droplets starting out larger than about 100 μm reach the ground in a few seconds before fully drying out, and typically land within 1 m from the source. The airborne lifetime of smaller droplets is strongly dependent on their initial size and relative humidity of the air. In practice, the upper limit for the airborne lifetime of small particles in enclosed spaces is constrained by

ventilation systems, which dilute the aerosol according to the number of air changes per hour: as low as 0.4 in residential buildings; ca 4 in office environments [66]; and ca 20 in airplanes [67]. While lingering in the air, particles will follow convection currents and travel considerable distances, fully analogous to the dispersion of smoke from a freshly lit cigarette whose smell is soon detected over large distances [7]. Even though the number density of particles will decrease with
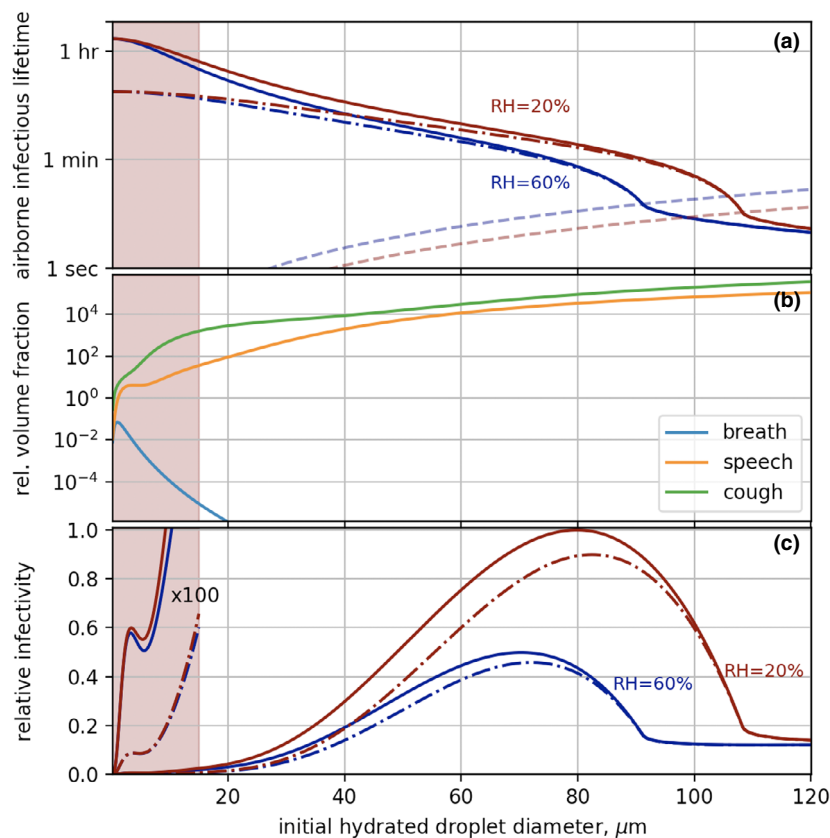
Fig. 4 *Airborne infectious lifetime, relative volume fraction and relative infectivity of respiratory droplets* vs. *initially hydrated diameter. The red-shaded area represents particle sizes capable of penetrating deep into the LRT after dehydration [124]. (a) The solid lines chart the time required for a droplet to fall 1.5 metres* vs. *its initial hydrated diameter at 20% and 60% relative humidity; the dashed lines indicate the time required to dehydrate. The lower humidity curve is typical of cooler locations in winter or in airplanes, while the higher humidity curve represents a typical upper limit for buildings to minimize risk of mould formation. Curves were calculated from eq. 13 in [125], but modified to account for air exchange and loss of aerosolized virus viability, which decays with a half-life of ca 1 hour [10]. The dot-dash curves correspond to an air exchange rate of four per hour, which is typical of office buildings [67]. (b) Size-dependent relative volume fraction of droplets generated per unit volume of expelled air by breathing, speaking and coughing, based on Table 6 of Pohlker et al. [40]. (c) The relative infectivity* vs. *droplet size curves correspond to the product of airborne infectious lifetime curves in panel (a) and the 'speech' curve in panel (b), assuming the same viral load per mL for all droplets. As in (a), the solid curves assume no ventilation, while the dot-dash curves correspond to four air changes per hour. The curves in the red-shaded area were scaled by a factor of 100 to reveal the extent to which ventilation can mitigate the risk of LRT infection.*

increasing distance from the source, there is no sharp distance cut-off. We also note that, analogous to smoke, their spread will not be effectively contained by simple plexiglass partitions.

The viral load in respiratory aerosol reflects the virion concentration in the fluid where the particles originate. For example, respiratory droplets can consist of saliva produced in the oral cavity, mucus generated in nasal passages, mucins generated by goblet cells in the bronchi and the larynx, or detergent-rich RTLF generated by cells lining the distal airways and respiratory bronchioles. Whereas the viral load in saliva was believed to be much lower than that in sputum, multiple studies suggest otherwise [68,69]. For example, the prevalence of ACE2 and TMPRSS2 entry factors in epithelial cells of glands and mucosae of the oral cavity implies that such cells are susceptible to infection by SARS-CoV-2, an observation borne out by the high viral loads found in saliva from an asymptomatic cohort [70]. Moreover, the viral content found in oro- and nasopharyngeal swabs is strongly overlapping [69], and though patient-to-patient variation spans at least seven orders of magnitude, the viral load can reach 10^9 copies per mL of fluid [69,71,72]. The presence of actively replicating infected cells in the oral cavity was also linked to mild symptoms such as loss of taste, but inversely correlated with systemic symptoms such as body aches and muscle pains [70]. These findings indicate that the oral cavity is an important site for SARS-CoV-2 infection and asymptomatic shedding, and confirm that oral fluid is a useful source of samples for diagnostic testing [68].

The probability that a droplet harbours virions is proportional to its initial volume, which scales as the cube of its diameter. Since the probability that a particle is inhaled by a bystander is proportional to the time it remains airborne after emission (Fig. 4a), the relative infection risk (Fig. 4c) scales as the product of its volume, airborne lifetime and the relative volume fraction represented by that droplet size (Fig. 4b), which can vary considerably depending on the activity that generated it.

Particles with diameters over *ca* 100 μm can carry tens or even hundreds of virions, but fall to the ground rather quickly and are less likely to be inhaled. At the other end of the size distribution, aerosols resulting from droplets smaller than 0.1 μm can linger in the air for many days, but since they are smaller than the diameter of a SARS-CoV-2 virion, they can be ignored. Consequently, droplet sizes between these two extremes are expected to pose the greatest risk. For example, dehydration of 45- and 15-μm droplets generate *ca* 15- and 5-μm aerosol particles, respectively. Though both particles can infect the nasopharynx and the upper airways (Fig. 5), the most common occurrence for SARS-CoV-2, only the smaller particle is able to descend into and infect the LRT [73,74], which exacerbates disease severity. The transmission risk ascribed to particles capable of causing a LRT infection, identified by the red-shaded region of Fig. 4, represents a small fraction of the total estimated transmission risk, which is consistent with the observation that most SARS-CoV-2 infections involve the upper respiratory tract (URT). According to Fig. 4c, droplets smaller than around 45 μm produce aerosols that linger in the air for many minutes and drift along with air currents. Since this size range carries with it significant transmission risk, regardless of humidity and air exchange rate, there is no sharp cut-off for what can be considered a safe distance from an unmasked carrier engaged in indoor speech.

As shown in Fig. 4b, the size distribution of emitted droplets depends on the activity that generates them. For example, breathing generates small droplets whose total liquid volume per litre of exhaled breath in a healthy person at rest is ≤15 fL/L. In contrast, the size distribution and volume of droplets emitted per litre of air expelled during a cough are many orders of magnitude greater. Given a bimodal lognormal size distribution with the most voluminous lobe centred at *ca* 100 μm [54,75], much of the liquid volume generated by a cough falls to the ground rather quickly. Nevertheless, the large number of smaller cough droplets will dehydrate before falling to the ground and remain airborne for minutes [6,58]. The size distribution for speech droplets is similar to that of cough, but its total liquid volume is less per litre of exhaled air. However, since speaking can be a continuous activity, and since a significant fraction of speech particles remain airborne for minutes, they accumulate in concentration and enhance the risk that some are inhaled by a bystander.

Despite the low liquid volume of breath droplets, they can still pose a hazard since breathing is an ongoing activity, and the airborne lifetime of breath aerosol spans hours. Thus, they can accumulate to levels limited only by the room ventilation rate
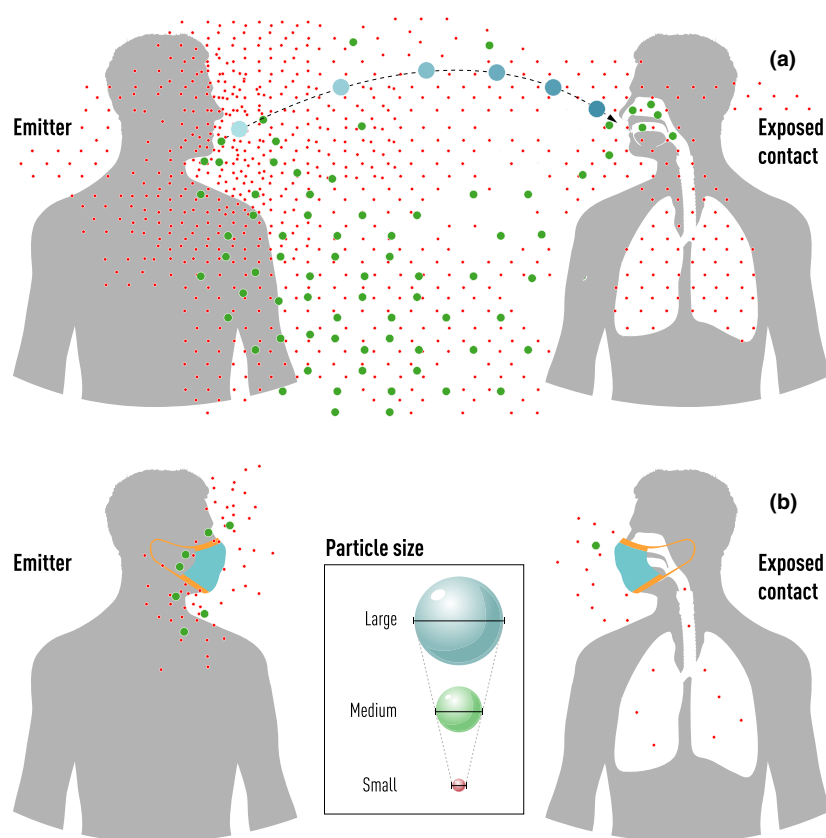
Fig. 5 *Emission of and exposure to respiratory droplets. (a) Left individual emits respiratory droplets of varying sizes, many of which remain airborne long enough to be inhaled into the upper and lower respiratory tracts of the exposed contact. Only very large droplets will follow a ballistic trajectory. (b) When masked, a small fraction of the emitter's droplets escape, mostly due to poor mask fit. The mask on the exposed contact filters out much of the remaining respiratory aerosol, but poor mask fit and small size of the dehydrated particles result in residual exposure [126].*

[34,74] and the timescale over which airborne virus remains viable, with SARS-CoV-2 degrading with a half-life of 1 hour in humid air [10]. Moreover, infection of the airways with SARS-CoV-2 in non-human primates resulted in a very large increase in breath droplet counts [47]. Consequently, the total aggregate of breath particles generated per hour in hospitalized patients can contain thousands or even millions of virions, particularly in severely ill patients [76,77]. Coupled with their small size, which allows them to penetrate deep into the LRT, and the difficulty to filter such particles without respirator masks, strongly elevated numbers of breath particles in hospital wards may be linked to the high levels of severe disease and death seen among healthcare workers during the early phase of the pandemic [78]. Note that in Fig. 4c, the risk of LRT infection (red-shaded region) is reduced modestly by increasing ambient humidity, but markedly by ensuring adequate air exchange.

What is the minimal infectious dose?

A key question relevant to all infectious diseases concerns the minimum number of pathogens required to cause illness. The dose that leads to a 50% probability of infection (ID50) is often equated with the minimum quantity needed to overwhelm the innate immune system. However, for respiratory virus transmission, there is a subtle but important distinction between ID50 and the minimal infectious dose: since the probability that any small respiratory aerosol contains more than a single viable virion is very low, the probability that multiple virions land in close proximity to one another on the very large epithelial surface of the

respiratory tract and overwhelm the local, innate immune system becomes vanishingly low.

In general, the probability (γ) that any inhaled virion will adhere to an ACE2 receptor, invade the cell and create progeny is small. However, this likelihood increases linearly with exposure, at least initially. This model of infection, which assumes zero cooperativity between virions, was employed in the classic study by Riley et al. of a large measles outbreak [79], and is interchangeably referred to as the 'single-hit model' (SHM) [80], the independent action hypothesis (IAH) [81] or the exponential model [82]. Note that the term quantum [79] is often used to describe the infectious dose, where 1 quantum equals $1/\gamma$ virions.

According to this model, the infection probability $P(n)$ upon inhaling n virions is given by.

$$P(n) = 1 - \exp(-n\gamma), \qquad (1)$$

which initially increases linearly with n. Below the ID50, and with minor adaptations, this model has been shown to be an excellent descriptor for the probability of sustained infection for a wide range of viral diseases [82], including SARS and MERS [83,84].

In the absence of synergistic effects between invading pathogens, how can we rationalize the empirically observed relationship between disease severity and infectious dose [85]? One plausible explanation is that disease severity is linked to the location of the infected host cell. For COVID-19 and many other respiratory virus infections, the most likely site of initial infection upon low-dose exposure is the epithelium of the URT. From there, infection can spread elsewhere, including the LRT, which will lead to increased disease severity [73,74,86,87]. When this migration occurs days after activation of the adaptive immune response, the severity of the LRT infection will be mitigated. In contrast, a high dose at the initial exposure increases the probability that, in addition to an URT infection, an independent infection initiates simultaneously in the LRT before the adaptive immune system is activated, significantly escalating disease severity.

According to this model, the number of inhaled aerosol particles required to reach ID50 is not small; however, this model also implies that a single infectious virion is capable of initiating

disease. There exists a preponderance of evidence supporting this notion. For example, early work on tuberculosis (TB) investigated transmission of the disease from humans to guinea pigs, whose only viable route involved airborne particles delivered to cages from a nearby patient ward through a ventilation system [88]. The authors of this study concluded that the disease initiates as a single primary tubercle delivered in a single airborne particle. Evidence supporting these important and far-reaching conclusions arose from linking the TB variant in infected animals to specific patients according to their respective drug resistance.

The type of infector–infectee pairing exploited in the TB study preceded the now widely adopted genetic sequence analysis of pathogens. SARS-CoV-2 possesses an efficient and tuneable proof-reading system that achieves relatively high replication fidelity [89] with a mutation rate of *ca* 10^{-6} per site per replication cycle [39]. As the disease progresses, random mutations cause the pathogen genome in an infected host to become slightly heterogeneous. Characterization of these variants can unveil correlations between sequences in infector–infectee pairs, which can be used to estimate the 'bottleneck size', that is the size of the pathogen population transferred from the infector that successfully created progeny in the infectee. The outcome of such analyses depends critically on the assumed fidelity of the sequencing. For example, deep sequencing analysis of Austrian superspreading events reported an average bottleneck size of *ca* 1000 virions [90]. However, reanalysis of the same data, but with a higher assumed sequencing error estimate, suggested that mutations in only 13 transmission pairs could be unambiguously linked and that for twelve of those, a bottleneck of a single virion best matched the data [91]. One particularly illuminating example highlighted in the Austrian study involved transmission between parents and their two adult children. Deep sequencing of the father's SARS-CoV-2 genome revealed 3.6% presence of a U allele in position 20,457 that was not present in the mother. Both of their children became infected, with this particular mutation represented at 25% in one and 100% in the other. The observation that a minor allele from the father was the dominant allele in one of their two children is fully consistent with the notion that a single inhaled virion is capable of initiating a new infection.

Vocalization at superspreading events

The concept of superspreaders, in which transmission from a single individual triggers numerous secondary cases, has long been recognized as a key factor in the spread of infectious disease. Indeed, the 20/80 rule, where 20% of the host population accounts for at least 80% of the transmission, applies to many infectious diseases [92,93], including COVID-19 [94]. Disease outbreaks are often characterized by superspreading events (SSEs), and many such events have been identified during the COVID-19 pandemic [95]. The first widely publicized SSE in the USA involved a conference in Boston that included a cocktail reception. Through phylogenetic analysis, as of 1 November 2020, more than 300,000 cases in the USA were traced back to this conference through two mutations, G26233T and C2416 [96]. This represents *ca* 3% of all infections in the USA at that time. Prevention of such superspreading events is therefore high on the list of priorities regarding measures to control the spread of COVID-19 [97]. Consequently, it is of key importance to identify characteristic signatures of SSEs. To that end, we briefly discuss several representative, well-documented outbreaks associated with SSEs (Table 1).

Two widely recognized common factors in all SSEs include the presence of at least one highly infectious host and, equally important, a suitable microenvironment with poor ventilation [98]. A third factor also emerges: loud vocalization. Indeed, the literature appears devoid of SSEs in settings such as libraries or movie theatres, where the first two factors may be met, but loud speech is minimal. However, cough droplets were possible vehicles in several SSEs where the index case was mildly symptomatic (Table 1). Note that some infectees do not develop symptoms, which implies the documented SSE transmission rates represent lower level estimates.

Invariably, SSEs involve the presence of a substantial number of people, which increases the likelihood that speech is loud, thereby raising the number of speech droplets [65]. Whereas little documentation is available detailing the loudness of speech in SSEs, the typical high level of background noise in environments such as a restaurant [99], an airliner [100] or a moving bus [101] suggests that the loudness of speech was likely above average. For the bar opening SSE [102], held indoors and with little ventilation, loud speech appears more than plausible. For the indoor 1-hr cycling fitness training class (Table 1), the instructor is reported as 'shouting instructions and encouragement from a podium > 6 ft removed from the 10-participants', all of whom became infected [55]. Similarly, well-documented choir events included loud vocalization [103,104] and, in particular for the Australian church singing events [105], provided strong evidence for the absence of physical contact or close proximity between the index case and infectees. Indeed, the airborne nature of disease transmission in such SSEs appears well above any reasonable doubt, and should come as no surprise considering that analogous airborne transmission has been well documented for influenza [106].

As noted above, singing generates high levels of small droplets that are released from the vocal folds and subsequently turn into aerosol. Such particles can penetrate deep into the lungs, which is known to be associated with more severe disease [73,74], and may speculatively be linked to the high fractions of severe disease and death associated with the choir events. However, the higher average age of infectees in these events (Table 1) relative to those in the bar opening or fitness class SSEs likely was a contributing factor as well. It is interesting to note that in the fitness class event, none of the participants escaped infection; that is, they must have received far more than the minimal infectious dose (see eq. 1). All of these secondary cases became symptomatic, with one requiring admission to an intensive care unit.

With some reasonable assumptions, including estimates of the volume of the enclosed space and the hourly volume of inspired air by participants, the observed probability that attendees in a superspreading event become infected can be linked to the amount of virus expelled by the index case. Such an analysis yielded an estimate of *ca* 1000 quanta for the Skagit Valley choir event [72], that is $1000/\gamma$ virions (eq 1), where γ is the probability that any single inhaled virion causes an infection.

How well can masks protect us?

Next to keeping physical distance, the use of face masks has become the most widely adopted measure to mitigate the spread of COVID-19. It is useful to divide masks into three categories: respirator masks, for example KN95, N95, N99 and FFP1-3; surgical masks; and generic cloth masks. During the early phase of the pandemic, respirator

Table 1 *Representative COVID-19 superspreading events*

Event setting	Number of people in attendance (excl. index case)	Age range in years (median)	Number of secondary infections (infection rate)	Number that developed symptoms	Duration	Estimated area in m^2	Droplet-generating activity	Index case symptomatic
Exercise class [55]	10	31–50 (37)	10 (100%)	10	1 hr.	38	Exercise and shouting	No
Choir, USA [72,103]	61	31–83 (69)	52 (85%)	52	2.5 hr.	NR	Singing and speaking	Yes
Choir, France [104]	27	35–86 (67)	18 (67%)	NR (11)[f]	2 hr.	45	Singing	No
Conference and reception [96]	175	NR	77 (44%)	NR	<48 hr.	NR	Speaking[a]	No
Bus [101]	68	NR	23 (34%)	20	~2 hr.	NR (40)[b]	Speaking[d]	No
Restaurant [99]	83	20–82 (54)	9 (11%)	9	~1 hr.	145	Speaking	No
Airliner [100]	217	56–68 (64)	15 (7%)	11	10 hr.	NR (258)[b]	Speaking[a]	Yes
Concert Hall, Australia [105]	320	NR	12 (4%)	12	2 hr.[c]	NR	Singing	No
Bar [102][e]	NR	18–64 (NR)	29	25	9 hr.	260	Speaking loudly[a]	Yes

NR, not reported (estimated).
[a]Assumed from the context.
[b]Estimated from the documented bus seat arrangement and airliner flight number.
[c]Two 1-hr concerts. All secondary cases sat within 1–15 metres from the index case, and were localized in 3 of the nearest 16 sectors in the concert hall.
[d]Obtained from private correspondence.
[e]Possible sources include one asymptomatic case (confirmed positive 1 day prior) and four mildly symptomatic cases (confirmed positive one day after event).
[f]Number of cases requiring hospitalization.

and surgical masks were in short supply in both Europe and the Americas, and were prioritized for medical frontline workers. By contrast, in many Asian countries, regular surgical masks have been widely used by the general public for more than a decade and are now credited with limiting the spread of SARS-CoV-2. Evidence regarding the effectiveness of masks and their shortcomings was presented in a recent review [107], but discussion of the utility of masks has become politically charged. Lost in much of this debate is that masks serve primarily two functions: limiting egress of potentially infectious respiratory droplets; and protection of the mask wearer by reducing ingress of virus-laden aerosol. Whereas the latter might be considered a personal choice, not limiting egress jeopardizes the health of others and therefore should be regulated in a civilized society.

Reducing egress is far simpler than ingress because respiratory droplets are emitted in a fully hydrated form that is approximately three times larger than the shrunken aerosol generated after dehydration in ambient air, and are therefore more easily captured by a face mask. Furthermore, cooling of expired air as it passes through a mask elevates its relative humidity beyond 100%, which causes the droplets to increase in size through nucleated condensation [108]. This increase in size further enhances the mask filtering efficiency, a factor widely ignored in tests of aerosol dispersals on mask materials or face masks on mannequins. Video recordings at the very early stage of the pandemic demonstrated that a face cover as simple as a washcloth blocks emission of more than 98% of speech-generated droplets [29]. However, an obvious shortcoming of both surgical and generic

masks is that a portion of expired air leaks around the mask with the accompanying droplets avoiding capture. The extent to which this happens depends on the fit of the mask, air resistance by the mask material and exhalation airflow. Double masking has been proposed as a solution to reduce such leakage [109] but makes breathing more difficult.

Protecting a mask wearer against ingress of aerosols is more difficult because of the small size of dehydrated respiratory aerosol; however, it is not as bad as one might think. Virion-containing droplets exiting the oral cavity also contain salt, mucus, lipids and other non-volatile components, and after dehydration remain highly hygroscopic. Consequently, when traversing a humid mask during ingress, respiratory aerosol will reacquire moisture and swell [108], thereby increasing the likelihood of their capture. This observation may explain why epidemiological evidence points to greater benefits of generic and surgical masks than expected on the basis of their limited dry particle filtering efficiency [110].

Masks may also minimize the possibility of self-inoculation of the LRT by one's own speech aerosol, a pathway for infection migration from the URT to the LRT that may accompany the more commonly considered micro-aspiration mechanism [111].

An additional benefit of masks may be the humidification of inspired air, which has been linked to both improved mucociliary clearance and the interferon-mediated innate immune response [112]. Natural fibers such as cotton and wool are particularly effective for such humidification [108], but all types of masks have this effect, albeit to different degrees [113].

SARS-CoV-2 can also trigger conjunctivitis or conjunctivitis-like signs and symptoms, but at an incidence of ≤1% for PCR-positive cases [114,115], the risk of primary infection through unprotected eyes is small. Importantly, conjunctiva infections are more commonly associated with severe disease [116], but could possibly arise from self-inoculation due to high exposure of the eyes to a carrier's own respiratory aerosol during the extended duration associated with severe disease.

Concluding remarks

Although now widely accepted, the use of personal respiratory protection against tuberculosis (TB)

was highly controversial when first included in the CDC Guidelines for preventing the transmission of *Mycobacterium tuberculosis* in healthcare facilities [117]. The CDC document stated, '*M. tuberculosis* is carried in airborne particles, or droplet nuclei, that can be generated when patients who have pulmonary or laryngeal TB sneeze, cough, speak, or sing. The particles are estimated to be 1–5 μm in size, and normal air currents can keep them airborne for prolonged time periods and spread them throughout a room or building'. The painstaking groundwork by Mills, Riley and Wells that led to these conclusions is lucidly described in a brief perspective by Riley [118], which highlights the reluctance of the medical community to come to grips with airborne TB transmission. It is perplexing that decades later, this same reluctance has persisted well into the current pandemic, despite strong evidence in support of airborne SARS-CoV-2 transmission.

One of the most challenging aspects of the COVID-19 pandemic is the high degree of presymptomatic and asymptomatic transmission [119,120], as highlighted in Table 1. Indeed, not only does the viral load in naso- and oropharyngeal swabs approach maximum levels around or soon after the onset of symptoms [69,71], but also once symptomatic, the ability of virions to infect a new host decreases with time [69,121,122]. As a consequence, a large and perhaps even dominant fraction of virus transmission takes place prior to the onset of COVID-19 symptoms [67,119,121], that is prior to coughing. Considering that breath droplets are generated in the lower respiratory tract and are unlikely to be rich in virus in the absence of clinical symptoms such as cough, speech droplets must represent a far more prevalent mode of presymptomatic and asymptomatic transmission of SARS-CoV-2.

A preponderance of evidence supports our conclusion that airborne transmission of SARS-CoV-2 is not only the dominant pathway for transmitting COVID-19, but unmasked speech in confined spaces represents the activity that poses the greatest risk to others. Since eating and drinking often take place indoors and typically involve loud speaking, it should come as no surprise that bars and restaurants have become the epicentre of multiple recent superspreading events [123]. Next to vaccination, mitigation strategies should emphasize the use of face masks when speaking and ensuring adequate ventilation to flush out

long-lived aerosols that might otherwise accumulate in closed environments and enhance the risk of more serious LRT infections.

The relatively high number and liquid volume of speech droplets, as well as their ability to remain airborne for many minutes, appears to be underappreciated by the public health community. Clearly, the significance of speech aerosol as a vehicle for virus transmission depends on the viability and concentration of virus in oral fluid. Whereas this concentration can be very high for SARS-CoV-2, it remains to be established whether viral transmission via speech particles is unique to COVID-19 or general to all respiratory viral diseases.

A final note: the SARS-CoV-2 virus is neither alive nor dead. It propagates primarily by hitching a ride inside an airborne respiratory particle from its host and then being inhaled into the respiratory tract of its next, unsuspecting victim. This virus respects no boundaries and, as of 8 April 2021, has infected an estimated 133 million people worldwide. Each infected individual becomes a Petri dish within which the virus mutates and, in classic Darwinian fashion, becomes more contagious over time. Indeed, its rapid evolution has produced numerous new variants that are inexorably becoming far more prevalent than their ancestor. A prudent and effective response to this and any pandemic would entail a unified effort to simultaneously minimize the case count in all countries, rich and poor. As a first step, it is crucial that the West embrace what the East has taught us all: face coverings limit the spread of respiratory viruses, and when compliance is high, either voluntarily or by mandate, the economic turmoil of shutdowns can be minimized or even avoided. It is perhaps helpful to be reminded of Voltaire's admonition: '*Don't let the perfect be the enemy of the good*'. If a carrier's mask results in 25% leakage of respiratory droplets, the risk that a bystander inhales particles from a masked carrier drops fourfold; if the exposed contact also wears a mask, with an estimated ingress filtering efficiency of 50%, the aggregate infection probability is reduced eightfold (Fig. 5). Such estimates suggest that *universal* masking, even with leaks, could strongly curb the spread of COVID-19.

Acknowledgements

Conflict of interest

The authors disclose no conflict of interest.

References

1 Ijaz MK, Brunner AH, Sattar SA, Nair RC, Johnsonlussenburg CM. Survival characteristics of airborne human coronavirus-229E. *J Gen Virol*. 1985;**66:**2743–8.

2 Makela MJ, Puhakka T, Ruuskanen O, Leinonen M, Saikku P, Kimpimaki M, *et al*. Viruses and bacteria in the etiology of the common cold. *J Clin Microbiol*. 1998;**36:**539–42.

3 Pfefferle S, Oppong S, Drexler JF, Gloza-Rausch F, Ipsen A, Seebens A, *et al*. Distant relatives of severe acute respiratory syndrome coronavirus and close relatives of human coronavirus 229E in bats, Ghana. *Emerg Infect Dis*. 2009;**15:** 1377–84.

4 Drosten C, Gunther S, Preiser W, van der Werf S, Brodt HR, Becker S, *et al*. Identification of a novel coronavirus in patients with severe acute respiratory syndrome. *N Engl J Med*. 2003;**348:**1967–76.

5 Wells WF. *Airborne contagion and air hygiene*. Cambridge: Harvard University Press; 1955.

6 Duguid JP. The size and the duration of air-carriage of respiratory droplets and droplet-nuclei. *J Hygiene*. 1946;**44:**471–9.

7 Prather KA, Marr LC, Schooley RT, McDiarmid MA, Wilson ME, Milton DK. Airborne transmission of SARS-CoV-2. *Science*. 2020;**370:**303–4.

8 CDC. Science brief: SARS-CoV-2 and potential airborne transmission; https://www.cdc.gov/coronavirus/2019-ncov/more/scientific-brief-sars-cov-2.html 2020.

9 Lednickya JA, Lauzardo M, Fan ZH, Jutla A, Tilly TB, Gangwar M, *et al*. Viable SARS-CoV-2 in the air of a hospital room with COVID-19 patients. *Int J Infect Dis*. 2020;**100:** 476–82.

10 van Doremalen N, Bushmaker T, Morris DH, Holbrook MG, Gamble A, Williamson BN, *et al*. Aerosol and surface stability of SARS-CoV-2 as compared with SARS-CoV-1. *N Engl J Med*. 2020;**382:**1564–7.

11 Matson MJ, Yinda CK, Seifert SN, Bushmaker T, Fischer RJ, van Doremalen N, *et al*. Effect of environmental conditions on SARS-CoV-2 stability in human nasal mucus and sputum. *Emerg Infect Dis*. 2020;**26:**2276–8.

12 Xiao SL, Li YG, Lei H, Lin CH, Norris SL, Yang XY, *et al*. Characterizing dynamic transmission of contaminants on a surface touch network. *Building Environ*. 2018;**129:**107–16.

13 Stephens B, Azimi P, Thoemmes MS, Heidarinejad M, Allen JG, Gilbert JA. Microbial exchange via fomites and implications for human health. *Curr Pollution Rep*. 2019;**5:**198–213.

14 Musher DM. Medical progress: how contagious are common respiratory tract infections? *N Engl J Med*. 2003;**348:** 1256–66.

15 Lewis D. COVID-19 rarely spreads through surfaces. So why are we still deep cleaning? *Nature.* 2021;**590:**26–8.

16 Dick EC, Jennings LC, Mink KA, Wartgow CD, Inhorn SL. Aerosol transmission of rhinovirus colds. *J Infect Dis.* 1987;**156:**442–8.

17 Asadi S, Gaaloul ben Hnia N, Barre RS, Wexler AS, Ristenpart WD, Bouvier NM. Influenza A virus is transmissible via aerosolized fomites. *Nat Comm.* 2020;**11:**4062.

18 Liu Y, Ning Z, Chen Y, Guo M, Liu Y, Gali NK, *et al.* Aerodynamic analysis of SARS-CoV-2 in two Wuhan hospitals. *Nature.* 2020;**582:**557–60.

19 Yu ITS, Li YG, Wong TW, Tam W, Chan AT, Lee JHW, *et al.* Evidence of airborne transmission of the severe acute respiratory syndrome virus. *N Engl J Med.* 2004;**350:**1731–9.

20 La Rosa G, Bonadonna L, Lucentini L, Kenmoe S, Suffredini E. Coronavirus in water environments: occurrence, persistence and concentration methods - A scoping review. *Water Res.* 2020;**179:**115899.

21 Graham KE, Loeb SK, Wolfe MK, Catoe D, Sinnott-Armstrong N, Kim S, *et al.* SARS-CoV-2 RNA in wastewater settled solids is associated with COVID-19 cases in a large urban sewershed. *Environ Sci Technol.* 2021;**55:**488–98.

22 Ahmed W, Angel N, Edson J, Bibby K, Bivins A, O'Brien JW, *et al.* First con firmed detection of SARS-CoV-2 in untreated wastewater in Australia: a proof of concept for the wastewater surveillance of COVID-19 in the community. *Sci Total Environ.* 2020;**728:**138764.

23 Bulfone TC, Malekinejad M, Rutherford GW, Razani N. Outdoor transmission of SARS-CoV-2 and other respiratory viruses: a systematic review. *J Infect Dis.* 2021;**223:**550–61.

24 Morawska L, Milton DK. It is time to address airborne transmission of COVID-19. *Clin Infect Dis.* 2020;**71:**2311–3.

25 Wells WF. On air-borne infection - Study II droplets and droplet nuclei. *Am J Hygiene.* 1934;**20:**611–8.

26 Loudon RG, Roberts RM. Droplet expulsion from respiratory tract. *Am Rev Respir Dis.* 1967;**95:**435–42.

27 Morawska L, Johnson GR, Ristovski ZD, Hargreaves M, Mengersen K, Corbett S, *et al.* Size distribution and sites of origin of droplets expelled from the human respiratory tract during expiratory activities. *J Aerosol Sci.* 2009;**40:**256–69.

28 Wells WF, Wells MW, Mudd S. Infection of air bacteriologic and epidemiologic factors. *Am J Pub Health Nations Health.* 1939;**29:**863–80.

29 Anfinrud P, Stadnytskyi V, Bax CE, Bax A. Visualizing speech-generated oral fluid droplets with laser light scattering. *N Engl J Med.* 2020;**382:**2061–3.

30 Bahl P, de Silva C, Bhattacharjee S, Stone H, Doolan C, Chughtai AA, *et al.* Droplets and aerosols generated by singing and the risk of COVID-19 for choirs. *Clin Infect Dis.* 2020;**72:**e639–41.

31 Alsved M, Matamis A, Bohlin R, Richter M, Bengtsson PE, Fraenkel CJ, *et al.* Exhaled respiratory particles during singing and talking. *Aerosol Sci Technol.* 2020;**54:**1245–8.

32 Bax A, Bax CE, Stadnytskyi V, Anfinrud P. SARS-CoV-2 transmission via speech-generated respiratory droplets. *Lancet Infect Dis.* 2020;**21:**318.

33 Stadnytskyi V, Bax CE, Bax A, Anfinrud P. The airborne lifetime of small speech droplets and their potential importance in SARS-CoV-2 transmission. *Proc Natl Acad Sci USA.* 2020;**117:**11875–7.

34 Fennelly KP. Particle sizes of infectious aerosols: implications for infection control. *Lancet Respir Med.* 2020;**8:**914–24.

35 Seminara G, Carli B, Forni G, Fuzzi S, Mazzino A, Rinaldo A. Biological fluid dynamics of airborne COVID-19 infection. *Rendiconti Lincei-Scienze Fisiche E Naturali.* 2020;**31:**505–37.

36 Bourouiba L. The fluid dynamics of disease transmission. *Ann Rev Fluid Mech.* 2021;**53:**473–508.

37 Morawska L, Tang JLW, Bahnfleth W, Bluyssen PM, Boerstra A, Buonanno G, *et al.* How can airborne transmission of COVID-19 indoors be minimised? *Environ Int.* 2020;**142:** 105832.

38 Chen WZ, Zhang N, Wei JJ, Yen HL, Li YG. Short-range airborne route dominates exposure of respiratory infection during close contact. *Build Environ.* 2020;**176:**106859.

39 Bar-On YM, Flamholz A, Phillips R, Milo R. SARS-CoV-2 (COVID-19) by the numbers. *eLife.* 2020;**9:**e57309.

40 Pöhlker M, Krüger O, Förster J, Berkemeier T, Elbert W, Fröhlich-Nowoisky J, *et al.* Respiratory aerosols and droplets in the transmission of infectious diseases. https://arxivorg/abs/210301188 2021.

41 Greenhalgh T, Jimenez JL, Prather KA, Tufekci Z, Fisman D, Schooley R. Ten scientific reasons in support of airborne transmission of SARS-CoV-2. *Lancet.* 2021;**397:**1603–5.

42 Wilson WC, Benumof JL. *Physiology of the airway. Benumof and Hagberg's airway management.* Philadelphia, PA: Saunders; 2013. p. 118–58.

43 Grasmeijer N, Frijlink HW, Hinrichs WLJ. An adaptable model for growth and/or shrinkage of droplets in the respiratory tract during inhalation of aqueous particles. *J Aerosol Sci.* 2016;**93:**21–34.

44 Weibel ER, Chapter VI. Geometry and dimensions of airways of the respiratory zone. In: Weibel ER, editor. *Morphometry of the human lung.* Berlin: Springer; 1963. p. 56–73.

45 Effros RM, Su J, Casaburi R, Shaker R, Biller J, Dunning M. Utility of exhaled breath condensates in chronic obstructive pulmonary disease: a critical review. *Curr Opin Pulm Med.* 2005;**11:**135–9.

46 Horvath I, Barnes PJ, Loukides S, Sterk PJ, Hogman M, Olin AC, *et al.* A European respiratory society technical standard: exhaled biomarkers in lung disease. *Europ Res J.* 2017;**49:**1600965.

47 Edwards DA, Ausiello D, Salzman J, Devlin T, Langer R, Beddingfield BJ, *et al.* Exhaled aerosol increases with COVID-19 infection, age, and obesity. *Proc Nat Acad Sci USA.* 2021;**118:**e2021830118.

48 Watanabe W, Thomas M, Clarke R, Klibanov AM, Langer R, Katstra J, *et al.* Why inhaling salt water changes what we exhale. *J Colloid Interface Sci.* 2007;**307:**71–8.

49 Ross BB, Gramiak R, Rahn H. Physical dynamics of the cough mechanism. *J Appl Physiol.* 1955;**8:**264–8.

50 Burger EJ, Macklem P. Airway closure - demonstration by breathing 100 percent O2 at low lung volumes and by N2 washout. *J Appl Physiol.* 1968;**25:**139.

51 Bake B, Larsson P, Ljungkvist G, Ljungstrom E, Olin AC. Exhaled particles and small airways. *Respir Res.* 2019;**20:**8.

52 Johnson GR, Morawska L. The mechanism of breath aerosol formation. *J Aerosol Med Pulmonary Drug Delivery.* 2009;**22:**229–37.

53 Holmgren H, Ljungstrom E, Almstrand AC, Bake B, Olin AC. Size distribution of exhaled particles in the range from 0.01 to 2.0 mu m. *J Aerosol Sci.* 2010;**41:**439–46.

54 Johnson GR, Morawska L, Ristovski ZD, Hargreaves M, Mengersen K, Chao CYH, *et al.* Modality of human expired aerosol size distributions. *J Aerosol Sci.* 2011;**42:**839–51.

55 Groves L, Usagawa L, Elm J, Low E, Manuzak A, Quint J, *et al*. Community transmission of SARS-CoV-2 at three fitness facilities — Hawaii, June–July 2020. *MMWR Morb Mortal Wkly Rep*. 2021;**70:**316–20.

56 Lendacki F, Teran R, Gretsch S, Fricchione M, Kerins J. COVID-19 Outbreak among attendees of an exercise facility — Chicago, Illinois, august–september 2020. *Morb Mortal Wkly Rep*. 2021;**70:**321–5.

57 Karlsson JA, Santambrogio G, Widdicombe J. Afferent neural pathways in cough and reflex bronchoconstriction. *J Appl Physiol*. 1988;**65:**1007–23.

58 Bourouiba L, Dehandschoewercker E, Bush JWM. Violent expiratory events: on coughing and sneezing. *J Fluid Mech*. 2014;**745:**537–63.

59 Moren F. *Aerosols in medicine: principles, diagnosis, and therapy*, 2nd edn. Amsterdam: Elsevier; 1993.

60 Burke RM, Killerby ME, Newton S, Ashworth CE, Berns AL, Brennan S, *et al*. Symptom profiles of a convenience sample of patients with COVID-19-United States, January-April 2020. *MMWR Morb Mortal Wkly Rep*. 2020;**69:**904–8.

61 Bourouiba L. A sneeze. *J Med*. 2016;**375:**E15.

62 Mittal R, Erath BD, Plesniak MW. Fluid dynamics of human phonation and speech. In: Davis SH, Moin P, editors. *Annual review of fluid mechanics*. 2013;**45:**437–67.

63 Abkarian M, Stone HA. Stretching and break-up of saliva filaments during speech: a route for pathogen aerosolization and its potential mitigation. *Physical Review Fluids*. 2020;**5:**102301. https://journals.aps.org/prfluids/abstract/10.1103/PhysRevFluids.5.102301.

64 Neubauer J, Zhang ZY, Miraghaie R, Berry DA. Coherent structures of the near field flow in a self-oscillating physical model of the vocal folds. *J Acoust Soc Am*. 2007;**121:**1102–18.

65 Asadi S, Wexler AS, Cappa CD, Barreda S, Bouvier NM, Ristenpart WD. Aerosol emission and superemission during human speech increase with voice loudness. *Sci Rep*. 2019;**9:**2348. https://www.nature.com/articles/s41598-019-38808-z.

66 ASHRAE. Ventilation for acceptable indoor air quality 2019.

67 Arons MM, Hatfield KM, Reddy SC, Kimball A, James A, Jacobs JR, *et al*. Presymptomatic SARS-CoV-2 infections and transmission in a skilled nursing facility. *N Engl J Med*. 2020;**382:**2081–90.

68 Wyllie AL, Fournier J, Casanovas-Massana A, Campbell M, Tokuyama M, Vijayakumar P, *et al*. Saliva or nasopharyngeal swab specimens for detection of SARS-CoV-2. *N Engl J Med*. 2020;**383:**1283–6.

69 Wölfel R, Corman VM, Guggemos W, Seilmaier M, Zange S, Müller MA, *et al*. Virological assessment of hospitalized patients with COVID-2019. *Nature*. 2020;**581:**465–9.

70 Huang N, Pérez P, Kato T, Mikami Y, Okuda K, Gilmore RC, *et al*. SARS-CoV-2 infection of the oral cavity and saliva. *Nat Med*. 2021;**27:**892–903.

71 To KK, Tsang OT, Leung WS, Tam AR, Wu TC, Lung DC, *et al*. Temporal profiles of viral load in posterior oropharyngeal saliva samples and serum antibody responses during infection by SARS-CoV-2: an observational cohort study. *Lancet Infect Dis*. 2020;**20:**565–74.

72 Miller SL, Nazaroff WW, Jimenez JL, Boerstra A, Buonanno G, Dancer SJ, *et al*. Transmission of SARS-CoV-2 by inhalation of respiratory aerosol in the Skagit Valley Chorale superspreading event. *Indoor Air*. 2021;**31:**314–23.

73 Gralton J, Tovey E, McLaws ML, Rawlinson WD. The role of particle size in aerosolised pathogen transmission: a review. *J Infection*. 2011;**62:**1–13.

74 Tellier R, Li Y, Cowling BJ, Tang JW. Recognition of aerosol transmission of infectious agents: a commentary. *BMC Infect Dis*. 2019;**19:**101.

75 Xie XJ, Li YG, Sun HQ, Liu L. Exhaled droplets due to talking and coughing. *J Royal Soc Interface*. 2009;**6:**S703–14.

76 Milton DK, Fabian MP, Cowling BJ, Grantham ML, McDevitt JJ. Influenza virus aerosols in human exhaled breath: particle size, culturability, and effect of surgical masks. *PLoS Pathog*. 2013;**9:**e1003205.

77 Ma J, Qi X, Chen H, Li X, Zhang Z, Wang H, *et al*. COVID-19 patients in earlier stages exhaled millions of SARS-CoV-2 per hour. *Clin Infect Dis*. 2020;**72:**e652–4.

78 Nioi M, Napoli PE, Lobina J, Fossarello M, d'Aloja E. COVID-19 and Italian healthcare workers from the initial sacrifice to the mrna vaccine: pandemic chrono-history, epidemiological data, ethical dilemmas, and future challenges. *Front Public Health*. 2021;**8:**1037.

79 Riley EC, Murphy G, Riley RL. Airborne spread of measles in a suburban elementary school. *Am J Epidemiol*. 1978;**107:**421–32.

80 Meynell GG, Stocker BAD. Some hypotheses on the aetiology of fatal infections in partially resistant hosts and their application to mice challenged with salmonella-paratyphi-B or salmonella-typhimurium by intraperitoneal injection. *J Gen Microbiol*. 1957;**16:**38–58.

81 Zwart MP, Hemerik L, Cory JS, de Visser J, Bianchi F, Van Oers MM, *et al*. An experimental test of the independent action hypothesis in virus-insect pathosystems. *Proc Royal Soc B-Biol Sci*. 2009;**276:**2233–42.

82 Haas CN. Microbial dose response modeling: past, present, and future. *Environ Sci Technol*. 2015;**49:**1245–59.

83 Watanabe T, Bartrand TA, Weir MH, Omura T, Haas CN. Development of a dose-response model for SARS coronavirus. *Risk Anal*. 2010;**30:**1129–38.

84 Adhikari U, Chabrelie A, Weir M, Boehnke K, McKenzie E, Ikner L, *et al*. A case study evaluating the risk of infection from middle eastern respiratory syndrome coronavirus (MERS-CoV) in a hospital setting through bioaerosols. *Risk Anal*. 2019;**39:**2608–24.

85 Guallar MP, Meirino R, Donat-Vargas C, Corral O, Jouve N, Soriano V. Inoculum at the time of SARS-CoV-2 exposure and risk of disease severity. *Int J Infect Dis*. 2020;**97:**290–2.

86 Zhao W, Zhong Z, Xie XZ, Yu QZ, Liu J. Relation between chest CT findings and clinical conditions of coronavirus disease (COVID-19) pneumonia: a multicenter study. *Am J Roentgenol*. 2020;**214:**1072–7.

87 Blain M, Kassin MT, Varble N, Wang XS, Xu ZY, Xu DG, *et al*. Determination of disease severity in COVID-19 patients using deep learning in chest X-ray images. *Diagn Interv Radiol*. 2021;**27:**20–7.

88 Riley RL, Shivpuri DN, Wittstadt F, Ogrady F, Sultan LU, Mills CC. Infectiousness of air from a tuberculosis ward - ultraviolet irradiation of infected air - comparative infectiousness of different patients. *Am Rev Respir Dis*. 1962;**85:**511–25.

89 Mercatelli D, Giorgi FM. Geographic and genomic distribution of SARS-CoV-2 mutations. *Front Microbiol*. 2020;**11:**1800.

90 Popa A, Genger JW, Nicholson MD, Penz T, Schmid D, Aberle SW, *et al.* Genomic epidemiology of superspreading events in Austria reveals mutational dynamics and transmission properties of SARS-CoV-2. *Sci Trans Med.* 2020;**12:**eabe2555.

91 Martin MA, Koelle K. Reanalysis of deep-sequencing data from Austria points towards a small SARS-COV-2 transmission bottleneck on the order of one to three virions. *bioRxiv.* 2021.

92 Woolhouse MEJ, Dye C, Etard JF, Smith T, Charlwood JD, Garnett GP, *et al.* Heterogeneities in the transmission of infectious agents: implications for the design of control programs. *Proc Natl Acad Sci USA.* 1997;**94:**338–42.

93 Lloyd-Smith JO, Schreiber SJ, Kopp PE, Getz WM. Superspreading and the effect of individual variation on disease emergence. *Nature.* 2005;**438:**355–9.

94 Adam DC, Wu P, Wong JY, Lau EHY, Tsang TK, Cauchemez S, *et al.* Clustering and superspreading potential of SARS-CoV-2 infections in Hong Kong. *Nat Med.* 2020;**26:**1714–9.

95 Majra D, Benson J, Pitts J, Stebbing J. SARS-CoV-2 (COVID-19) superspreader events. *J Infect.* 2021;**82:**36–40.

96 Lemieux JE, Siddle KJ, Shaw BM, Loreth C, Schaffner SF, Gladden-Young A, *et al.* Phylogenetic analysis of SARS-CoV-2 in Boston highlights the impact of superspreading events. *Science.* 2021;**371:**588–96.

97 Frieden TR, Lee CT. Identifying and interrupting superspreading events-implications for control of severe acute respiratory syndrome coronavirus 2. *Emerg Infect Dis.* 2020;**26:**1061–6.

98 Buonanno G, Morawska L, Stabile L. Quantitative assessment of the risk of airborne transmission of SARS-CoV-2 infection: prospective and retrospective applications. *Environ Int.* 2020;**145:**10.

99 Lu JY, Gu JN, Li KB, Xu CH, Su WZ, Lai ZS, *et al.* COVID-19 outbreak associated with air conditioning in restaurant, Guangzhou, China, 2020. *Emerg Infect Dis.* 2020;**26:**1628–31.

100 Khanh NC, Thai PQ, Quach HL, Thi NAH, Dinh PC, Duong TN, *et al.* Transmission of SARS-CoV-2 during long-haul flight. *Emerg Infect Dis.* 2020;**26:**2617–24.

101 Shen Y, Li CW, Dong HJ, Wang Z, Martinez L, Sun Z, *et al.* Community outbreak investigation of SARS-CoV-2 transmission among bus riders in Eastern China. *JAMA Int Med.* 2020;**180:**1665–71.

102 Sami S, Turbyfill CR, Daniel-Wayman S, Shonkwiler S, Fisher KA, Kuhring M, *et al.* Community transmission of SARS-CoV-2 associated with a local bar opening event — Illinois, February 2021. *MMWR Morb Mortal Wkly Rep.* 2021;**70:**528–32.

103 Hamner L, Dubbel P, Capron I, Ross A, Jordan A, Lee J, *et al.* High SARS-CoV-2 attack rate following exposure at a choir practice - Skagit County, Washington, March 2020. *Mmwr-Morbidity Mort Weekly Rep.* 2020;**69:**606–10.

104 Charlotte N. High rate of SARS-CoV-2 transmission due to choir practice in France at the beginning of the COVID-19 pandemic. *J Voice.* 2020. https://doi.org/10.1016/j.jvoice.2020.11.029.

105 Katelaris A, Wells J, Clark P, Norton S, Rockett R, Arnott A, *et al.* Epidemiologic evidence for airborne transmission of SARS-CoV-2 during Church Singing, Australia, 2020. *Em Infect Dis.* 2021;**27:**1677–80.

106 Moser MR, Bender TR, Margolis HS, Noble GR, Kendal AP, Ritter DG. Outbreak of influenza aboard a commercial airliner. *Am J Epidemiol.* 1979;**110:**1–6.

107 Howard J, Huang A, Li Z, Tufekci Z, Zdimal V, van der Westhuizen H-M, *et al.* An evidence review of face masks against COVID-19. *Proc Natl Acad Sci USA.* 2021;**118:**e2014564118.

108 Zangmeister CD, Radney JG, Staymates ME, Vicenzi EP, Weaver JL. Hydration of hydrophilic cloth face masks enhances the filtration of nanoparticles. *ACS Applied Nano Materials.* 2021;**4:**2694–701.

109 Brooks J, Beezhold D, Noti J, Coyle J, Derk R, Blachere F, *et al.* Maximizing fit for cloth and medical procedure masks to improve performance and reduce SARS-CoV-2 transmission and exposure. *MMWR Morb Mortal Wkly Rep.* 2021;**70:**254–7.

110 Gandhi M, Beyrer C, Goosby E. Masks do more than protect others during COVID-19: reducing the inoculum of SARS-CoV-2 to protect the wearer. *J General Int Med.* 2020;**35:**3063–6.

111 Hou YXJ, Okuda K, Edwards CE, Martinez DR, Asakura T, Dinnon KH, *et al.* SARS-CoV-2 reverse genetics reveals a variable infection gradient in the respiratory tract. *Cell.* 2020;**182:**429.

112 Kudo E, Song E, Yockey LJ, Rakib T, Wong PW, Homer RJ, *et al.* Low ambient humidity impairs barrier function and innate resistance against influenza infection. *Proc Natl Acad Sci USA.* 2019;**116:**10905–10.

113 Courtney JM, Bax A. Hydrating the respiratory tract: an alternative explanation why masks lower severity of COVID-19. *Biophys J.* 2021;**120:**994–1000.

114 Peng M, Dai JN, Sugali CK, Rayana NP, Mao WM. The role of the ocular tissue in SARS-CoV-2 transmission. *Clin Ophthalmol.* 2020;**14:**3017–24.

115 Chen LW, Deng CH, Chen XH, Zhang X, Chen B, Yu HM, *et al.* Ocular manifestations and clinical characteristics of 535 cases of COVID-19 in Wuhan, China: a cross-sectional study. *Acta Ophthalmol.* 2020;**98:**E951–9.

116 Loffredo L, Pacella F, Pacella E, Tiscione G, Oliva A, Violi F. Conjunctivitis and COVID-19: a meta-analysis. *J Med Virol.* 2020;**92:**1413–4.

117 Fennelly KP. Personal respiratory protection against mycobacterium tuberculosis. *Clin Chest Med.* 1997;**18:**1–18.

118 Riley RL. What nobody needs to know about airborne infection. *Am J Res Crit Care Med.* 2001;**163:**7–8.

119 Rothe C, Schunk M, Sothmann P, Bretzel G, Froeschl G, Wallrauch C, *et al.* Transmission of 2019-nCoV infection from an asymptomatic contact in Germany. *N Engl J Med.* 2020;**382:**970–1.

120 Oran DP, Topol EJ. Prevalence of asymptomatic SARS-CoV-2 infection. *Ann Intern Med.* 2020;**173:**362–7.

121 He X, Lau EHY, Wu P, Deng XL, Wang J, Hao XX, *et al.* Temporal dynamics in viral shedding and transmissibility of COVID-19. *Nat Med.* 2020;**26:**672–5.

122 Bullard J, Dust K, Funk D, Strong JE, Alexander D, Garnett L, *et al.* Predicting infectious severe acute respiratory syndrome coronavirus 2 from diagnostic samples. *Clin Infect Dis.* 2020;**71:**2663–6.

123 Chang S, Pierson E, Koh PW, Gerardin J, Redbird B, Grusky D, *et al.* Mobility network models of COVID-19 explain inequities and inform reopening. *Nature.* 2021;**589:**82–7.

124 Roy CJ, Milton DK. Airborne transmission of communicable infection - The elusive pathway. *N Engl J Med.* 2004;**350:** 1710–2.

125 Netz R. Mechanisms of airborne infection via evaporating and sedimenting droplets produced by speaking. *J Phys Chem B.* 2020;**124:**7093–101.

126 Milton DK. A rosetta stone for understanding infectious drops and aerosols. *J Pediatric Infect Dis Soc.* 2020;**9:**413–5.

Correspondence: Philip Anfinrud and Adriaan Bax, Laboratory of Chemical Physics, NIDDK, National Institutes of Health, Bethesda, MD 20892-0520, USA.
(e-mails: philipa@intra.niddk.nih.gov and bax@nih.gov).■